Energy Engineering

Tech Science Press

DOI: 10.32604/EE.2021.014535

ARTICLE

Multi-Scale Superhydrophobic Anti-Icing Coating for Wind Turbine Blades

Jiangyong Bao[1], Jianjun He[1,*], Biao Chen[2], Kaijun Yang[1], Jun Jie[2], Ruifeng Wang[1] and Shihao Zhang[2]

[1]School of Energy and Power Engineering, Changsha University of Science and Technology, Changsha, 410114, China

[2]Guodian Longyuan Jiangyong Wind Power Co., Ltd., Changsha, 410000, China

[*]Corresponding Author: Jianjun He. Email: hejianjun@csust.edu.cn

Received: 07 October 2020 Accepted: 31 December 2020

ABSTRACT

As a surface functional material, super-hydrophobic coating has great application potential in wind turbine blade anti-icing, self-cleaning and drag reduction. In this study, ZnO and SiO_2 multi-scale superhydrophobic coatings with mechanical flexibility were prepared by embedding modified ZnO and SiO_2 nanoparticles in PDMS. The prepared coating has a higher static water contact angle (CA is 153°) and a lower rolling angle (SA is 3.3°), showing excellent super-hydrophobicity. Because of its excellent superhydrophobic ability and micro-nano structure, the coating has good anti-icing ability. Under the conditions of −10°C and 60% relative humidity, the coating can delay the freezing time by 1511S, which is 10.7 times slower than the normal freezing time. More importantly, due to the mechanical properties provided by SiO_2 and the synergistic effect of micro-nano particles, the coating has excellent mechanical durability. After 10 wear tests, the contact angle of the coating is still as high as 141° and the rolling angle is 6.8°. This research provides a theoretical reference for the preparation of a mechanically stable coating with a simple preparation process, as well as a basic research on the anti-icing behavior of the coating.

KEYWORDS

Mechanical flexibility; ZnO; SiO_2; multi-scale; superhydrophobic

1 Introduction

With the rapid development of wind power technology, various problems faced by wind turbines during the operation are also emerging. Among them, the problem of wind turbine blade icing is one of the focuses of current research in the wind power industry [1,2]. For the icing of wind turbine blades, coating is currently one of the most popular solutions. In recent years, with the continuous development of science, related materials in the superhydrophobic field have emerged one after another, which has attracted widespread attention of experts and scholars at home and abroad. Normally, superhydrophobic surface refers to the surface with CA > 150°, SA < 10° [3] (CA:Contact angle; SA:Sliding angle). Due to superhydrophobic surface extreme hydrophobicity and self-cleaning properties, it has very important applications in self-cleaning [4], deicing [5], antifreeze [6], oil-water separation [7], corrosion protection [8] and so on. There have been 24 years of research history since the lotus leaf phenomenon was discovered in 1996, but there still exists many problems in its practical application, mainly in the poor mechanical stability of the superhydrophobic surface and unstable surface chemical properties [9]. The main reason for this problem is that the superhydrophobicity of the artificial superhydrophobic surface mainly relies on the construction

of micro-nano structures and low surface energy substances [10]. Since the micro-nano structure is very fragile, it is very easy to be damaged by external forces, which damages the Cassie-Baxter model and affects the hydrophobic properties of the surface [11]. At present, the chemical properties of the surface of superhydrophobic materials are very unstable. The main reason is that under the influence of external acid, alkali and other factors, the micro-nano structure and surface energy substances may undergo physical and chemical changes, making the surface superhydrophobic properties reduce or even be lost [12].

In view of the problems mentioned above which are faced by superhydrophobic surfaces, researchers have carried out many related researches. Dai et al. [13] fabricated three-dimensional layered ZnO nanostructures on PDMS substrates through PDMS pouring process and solution growth procedures, and found that the ZnO nanostructures grown on layered PDMS substrates have a great influence on the surface wetting behavior. Zhou et al. [14] controlled the ratio of ZnO to epoxy resin so that the ZnO particles were not completely covered, forming a clustered ZnO coating. After modification with stearic acid, the coating has excellent superhydrophobicity and exhibits excellent wear resistance. Zhang et al. [15] combined the rough structured SiO_2 film with low surface energy and durable PDMS by electrodeposition, and built a corrosion-resistant coating on low-carbon steel with good resistance corrosion performance. Wang et al. [16] use PDMS, SiO_2, $CaCO_3$, etc., to only back the composite coating, which can be directly applied to different substrates and has certain anti-corrosion performance and self-healing ability. Lu et al. [17] used perfluorosilane fluorinated ethanol solution to wrap TiO_2 nanoparticles to form a suspension sprayed or brushed onto the substrate to obtain a superhydrophobic coating, and developed a "paint + adhesive" adhesive. The method was to overcome the weak mechanical properties of the superhydrophobic surface. Li et al. [18] proposed a new method of "glue + powder". By embedding various functional micro-nano particles to realize the functionalization of superhydrophobic surfaces, the relationship between the intrinsic wettability of embedded particles and the wettability of superhydrophobic surfaces was studied. Through experiments, it was found that there is no obvious connection between the two. The size and level of the microstructure are considered to be the decisive factors for liquid hydrophobicity. That is, smaller and coarse particles promote better hydrophobicity. Kim et al. [19] used acrylate-polyurethane (PU) adhesives combined with fluorinated SiO_2 nanoparticles to prepare a mechanically stable superhydrophobic coating. Through experiment, they found that the binder plays a key role in controlling surface roughness and superhydrophobicity through the capillary mechanism. Zhang et al. [20] sprayed a mixture of ZnO and epoxy on the surface of the substrate. Then they used stearic acid and acetic acid solutions to roughen the surface of the coating to form a micro-nano structure and reduce surface energy to prepare a mechanically stable and wear-resistant superhydrophobic coating.

Inspired by the above research, a superhydrophobic coating with mechanically flexible ZnO/SiO_2 multi-scale micro/nano structure was directly constructed by the embedding method. This method mainly uses SiO_2 to effectively improve the mechanical properties of the coating, heating and weather resistance, and corrosion resistance. In addition, ZnO is easy to handle and directly constructs low surface energy micro-nano structures. Based on PDMS, a multi-scale micro nano superhydrophobic coating was constructed. Compared with previous studies, the preparation process of the coating is very simple, and the coating has excellent mechanical stability and superhydrophobicity by modifying the two kinds of particles. At the same time, because the coating has certain self-cleaning, anti-freezing and deicing ability, it can effectively alleviate the icing problem of wind turbine blades and improve the power generation time of wind turbines [21].

2 Materials and Methods

2.1 Materials

Nano Zno (20–30 nm), nano SiO_2 (100–300 nm), PDMS and its curing agent, FAS-17, ethanol (AR), acetic acid, and STA.

2.2 Coating Preparation

2.2.1 Fluorination Modification of ZnO

A certain amount of ZnO was put into 10 ml of ethanol mixed solution containing different amounts of FAS-17, and the mixture was vigorously stirred for 2 h in an oil bath at 45°C. Then the obtained ZnO was repeatedly washed in an ethanol solution and dried at 120°C for 2 h to obtain FAS-ZnO particles. As we all know, $-CF_3$ in the fluorine-containing group has extremely low surface energy. FAS-17 grafts $ZnOH^+$ ions, so that the hydroxyl groups on the surface of ZnO are replaced by FAS molecules.

$$Zn^{2+} + 2OH^- \rightarrow Zn(OH)_2 \tag{1}$$

$$Zn(OH)_2 \rightarrow ZnO + H_2O \tag{2}$$

$$Zn(OH)_2 + CF_3 - (CF_2)_5 - CH_2 - CH_2 - Si - (OCH_2CH_3)_3 \rightarrow CF_3 - (CF_2)_5 - CH_2 - CH_2 - Si - (O - ZnOH)_3 \tag{3}$$

2.2.2 Hydrophobic Modification of SiO_2

Put a certain amount of SiO_2 into 50ML absolute ethanol solution, ultrasonically treat for 5 min, add 1ML OTS, and magnetically stir in a 60°C water bath for 2 h to obtain modified SiO_2 particles. The obtained modified SiO_2 particles are washed twice in absolute ethanol and dried to obtain finished superhydrophobic SiO_2 particles. As shown in Fig. 1, through the modification of OTS, a carbon chain of 18 carbon atoms is added to the SiO_2 molecule, which increases its hydrophobic chain length and reduces hydrophilic groups, making it exhibit excellent hydrophobicity.

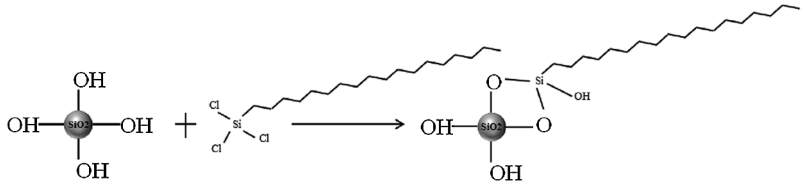

Figure 1: Modified SiO_2 molecule and its reaction formula

2.2.3 Construction of ZnO/SiO_2 Multi-Scale Superhydrophobic Coating

In the first step, PDMS and curing agent are mixed in a ratio of 10:1, and then uniformly coated on the glass substrate to form a layered liquid film with a thickness of about 3.5 mm. In the second step, ZnO and SiO_2 are mixed in a certain proportion, and they are evenly sprinkled on the formed layered liquid through a sieve until the liquid film is covered by ZnO and SiO_2, and dried in a drying oven at 80°C for 4 h. Finally, the coating was taken out, immersed in a 5 wt% stearic acid solution to further roughen the coating surface, and then put into a 20 wt% acetic acid/ethanol solution to further reduce its surface energy [22]. Finally, it was dried at room temperature for 1 h to form a ZnO/SiO_2 multi-scale superhydrophobic coating. The preparation process of ZnO/SiO_2 multi-scale superhydrophobic coating is shown in Fig. 2.

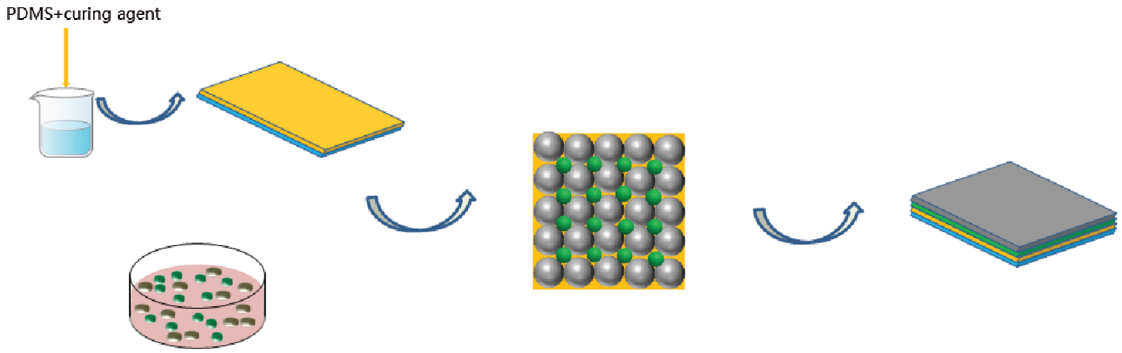

Figure 2: Preparation process of ZnO/SiO_2 multi-scale superhydrophobic coating

2.3 Characterizations

Under the scanning electron microscope (SEM, QUANTA250, USA), the morphology of the coating was characterized. Under the optical microscope (OM, 200mat, USA), the surface difference before and after wear was characterized. Fourier transform infrared spectroscopy (FTIR, Nicolet iS10, USA) was used to study the functional group changes of the modified nanoparticles. The water CA was determined with OCA15 contact angle analyzer (Data-physics, Germany). In order to simulate the icing situation in a high-altitude, low-temperature and high-humidity environment, the actual anti-icing performance of the coating was tested using a methyl blue solution under an artificial freezing environment of −10°C and 60% relative humidity. The experiment included: ice experiment and dynamic icing experiment. A 50 g weight was used to apply gravity to the coating, and a wear test of the coated sandpaper was performed on the SiC sandpaper to verify the mechanical stability of the coating. The self-cleaning ability was tested by putting the coating sample into the methyl blue solution and then taking it out.

3 Results and Discussion

3.1 Microstructure and Chemical Composition of the Coating Surface

3.1.1 Hydrophobicity of Fluorinated ZnO Nanoparticles

Hydrophobic ZnO nanoparticles are conducive to effective combination with PDMS substrates. Fig. 3 shows the wettability of treated and untreated ZnO nanoparticles. The unmodified ZnO nanoparticles are completely hydrophilic due to their high surface free energy without any hydrophobic effect. However, when the water droplets fall on the surface of the fluorinated modified ZnO particle powder, the water droplet is spherical and difficult to wet on the surface of the modified ZnO particle powder. This phenomenon shows that ZnO has been modified to become hydrophobic particles, and its surface free energy is reduced. This phenomenon is mainly due to the modification of ZnO nanoparticles by FAS-17.

(a) (b)

Figure 3: Hydrophobic effect diagram of ZnO powder: (a) fluorination treatment, and (b) untreated

Due to the existence of C-F and C-H groups, FAS-17 can not only reduce the free energy on the surface of its ZnO nanoparticles, but also make it more soluble in organic solvents and avoid the occurrence of nanoparticle agglomeration [23,24]. The CA of FAS on a smooth plane is 109°, which has good hydrophobicity, and its molecules are easy to modify on the hydroxyl-rich surface [25,26]. Fig. 4 shows the FTIR spectrum of FAS-ZnO. The band at 1065 cm^{-1} is attributable to the asymmetric stretching vibration of the Si-O-Zn material, which proves the dehydration reaction between the hydrolyzed Fas molecules and the ZnO particles. FAS-ZnO has three peaks at 1128, 1210 and 1150 cm^{-1}, which are attributed to the stretching vibration of $-CF_2$ and $-CF_3$ groups, indicating that fluorinated ZnO particles have been successfully synthesized.

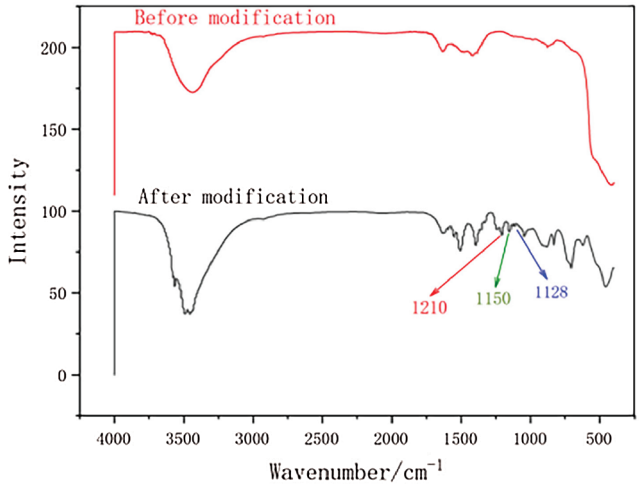

Figure 4: FTIR spectrum of FAS-ZnO

3.1.2 Microstructure of Coating Surface

The natural superhydrophobic surface micro-rough structure and low surface energy chemical composition of "lotus leaf effect" and "rose petal effect", among which level difference and microscopic gap size are the key to regulating the water adhesion behavior of superhydrophobic surface [27,28]. It can be seen that the roughness of the coating surface provided by the micro-nano structure is important for the ZnO/SiO_2 multi-scale superhydrophobic coating. It can be seen from Figs. 5a and 5b that the ZnO/SiO_2 multi-scale superhydrophobic coating has a unique surface structure. The coated ZnO and SiO_2 nanoparticles adhere to the PDMS substrate to form a high specific surface. The rough hilly porous structure effectively reduces the area of the coating and reduces the surface energy of the coating. At the same time, the secondary structure can be observed from Figs. 5c and 5d, which indicates that the ZnO and SiO_2 nanoparticles added are not completely covered by the PDMS substrate, only the particles adhere to the PDMS substrate. Since the droplets drop on the surface of the coating, the air is trapped in the cavities on the surface of the layered rough structure, forming a solid-liquid-gas three-phase contact state, and it is difficult for the droplets to penetrate into the micro-nano porous structure [29,30]. The water adhesion behavior is also consistent with the low water adhesion superhydrophobic state of the Cassie-Baxter wetting model [31,32]. At the same time, SiO_2 particles are modified by OTS, adding a carbon chain of 18 carbon atoms, reducing the hydroxyl hydrophilic groups on the surface; ZnO particles are modified by FAS-17 fluorination to make the hydroxyl groups on the surface of ZnO hydrophilic. The groups are replaced by FAS molecules. By modifying ZnO and SiO_2, the surface energy of the coating is

further reduced and the superhydrophobic ability is further enhanced. Therefore, the surface can exhibit a surface state of high CA (153°), low SA (3.3°) and low adhesion.

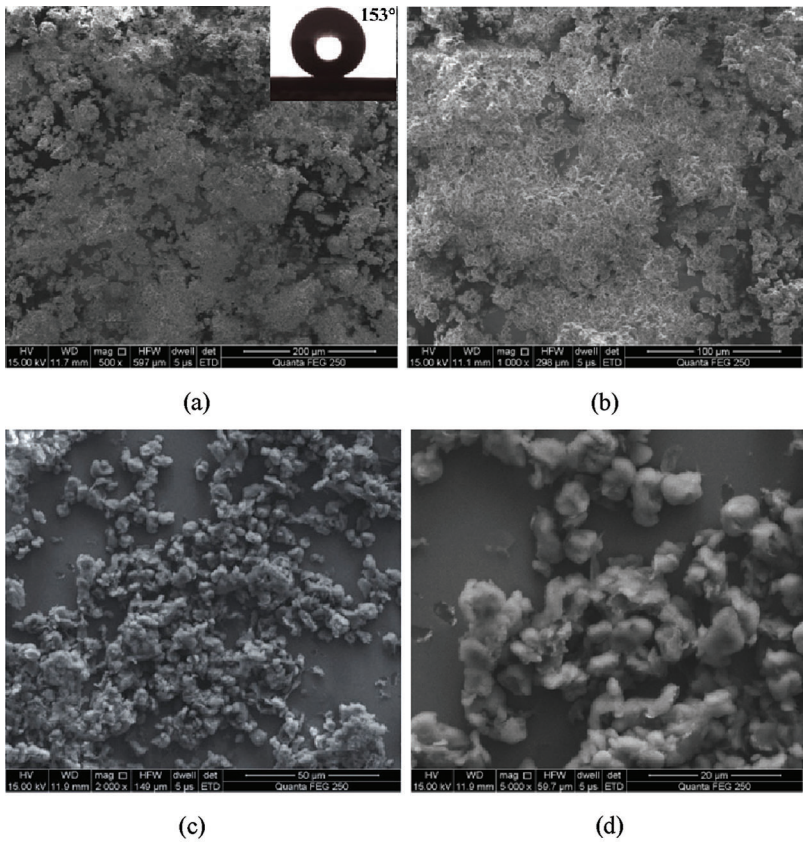

Figure 5: SEM image of ZnO/SiO_2 multi-scale superhydrophobic coating: (a) 500x enlargement, (b) 1000x enlargement, (c) 2000x partial enlargement, and (d) 5000x partial enlargement

3.2 Superhydrophobic Properties, Self-Cleaning

The wettability of a superhydrophobic surface is mainly determined by the microstructure and chemical composition of the surface. It reflects its performance by measuring the CA and SA of water droplets on its surface [33]. In order to better understand the influence of the morphology of ZnO/SiO_2 nanoparticles on the wettability of the prepared multi-scale superhydrophobic coating, we analyzed and discussed the relationship between nanoparticles and wettability. Although the CA of PDMS with a smooth and pure surface is 114°, which can bring a certain degree of hydrophobicity to it, the addition of modified ZnO and SiO_2 nanoparticles can further enhance the hydrophobicity and improve the physical properties of PDMS itself. This is mainly the microscopic rough structure caused by F-ZnO and modified SiO_2 nanoparticles. As shown in Fig. 6a, the surface is immersed in water, the coating is surrounded by an air cushion with strong light reflection, and it proved to be superhydrophobic. As shown in Fig. 6b, by putting the ZnO/SiO_2 coating sample in the methyl blue solution for a period of time and then taking it out, there is no difference in the surface, which proves that it has a certain self-cleaning ability.

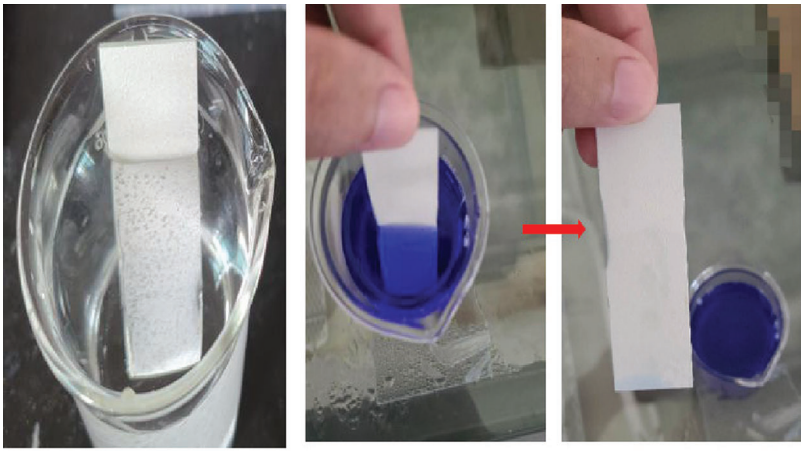

Figure 6: Coating performance test: (a) coating wettability test, and (b) schematic diagram of methyl blue solution test

3.3 Anti-Snow and Icing Performance

As we all know, freezing on the coating surface is greatly affected by temperature [34]. In addition to the influence of temperature, the characteristics of the icing surface, surface roughness and surface energy have a greater influence on the surface icing phenomenon. Under the action of adsorption force, ice crystals can adhere to the icy surface and deposit continuously. The size of this adsorption force depends on the wettability between ice crystals and the frozen surface. If it is a hydrophobic surface with low surface energy, it can make the ice crystal and the surface in a non-wetting state, which can greatly reduce the adsorption force to the ice crystal and prevent freezing [35]. The surface roughness of the coating makes the contact of water and the coating surface into a non-wetting state due to the presence of a part of the entrained air [36]. At the same time, the solid-liquid-gas three-phase contact state greatly reduces the heat transfer efficiency of the coating and prolongs the time for water to freeze.

Through the icing experiment at −10°C and 60% relative humidity, the actual anti-icing performance of the ZnO/SiO_2 coating in a simulated high altitude, low temperature and high humidity environment was tested. As show in Fig. 7a, the prolonged freezing time of water droplets stained with methylene blue on ZnO/SiO_2 coated and uncoated glass slides was tested, and the actual data of the two were compared in the icing experiment. By controlling the temperature of the freezer, the surface temperatures of the coated and uncoated glass slides are both at −10°C. On the uncoated glass slides, the water droplets began to freeze after 10 s, and began to freeze locally after 55 s and completely frozen after 156 s. The water droplets on the surface of the coating began to become opaque from 833S to the 1263S. The test tube was used for testing. Only the surface was frozen, while the inside was still liquid. The water droplets on the surface of the 1667S coating were completely frozen. The surface of the layer is 10.7 times slower. At the same time, in order to test the performance stability of the coating under extreme temperature conditions, icing experiments at −2°C and −20°C were carried out. As shown in Fig. 7b, at −2°C, the uncoated glass slide was frozen at 337S, and the coated glass slide was frozen at 2583S, which was delayed for 37 min. As shown in Fig. 7c, at −20°C, the uncoated glass slide was frozen at 31S, and the coated glass slide was frozen at 155S, which was delayed for 2 min.

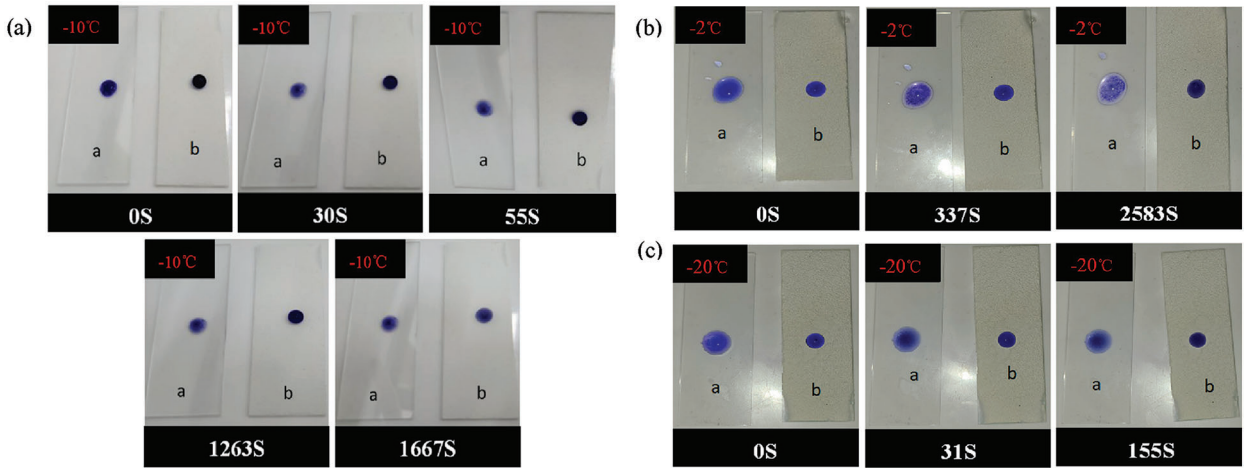

Figure 7: Process diagram of icing experiment (a is uncoated, b is coated): (a) process chart of −10°C icing test, (b) process chart of −2°C icing test, and (c) process chart of −20°C icing test

A self-made device was used to carry out the coating dynamic icing experiment, as shown in Fig. 8. First, let the water mist fall on the ZnO/SiO_2 coated and uncoated glass slides at a certain speed at a position about 10 cm away from the coating. Then, compare the icing conditions of both sides. In an environment of −10°C, the uncoated glass slide began to freeze gradually in about 6 min, and no ice was formed on the surface of the ZnO/SiO_2 coating, which further indicated that the ZnO/SiO_2 excellent anti-icing performance of the coating. The result is shown in Fig. 9.

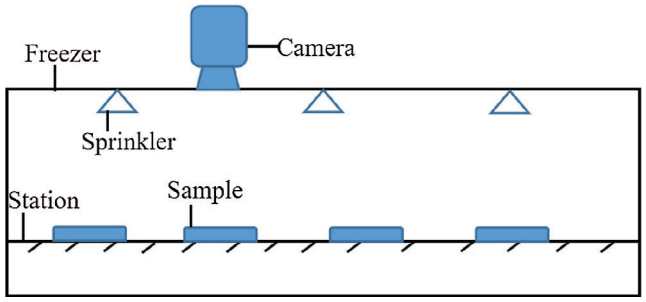

Figure 8: Schematic diagram of dynamic icing experiment device

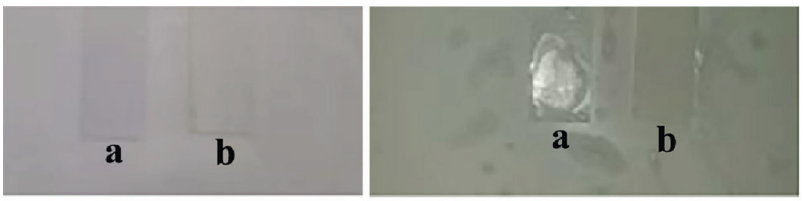

Figure 9: Comparison of dynamic icing experiments: (a) before freezing, and (b) after freezing

As expected, the ZnO/SiO_2 coating can delay water condensation for a long time and has good anti-icing properties. The coating has such good anti-icing performance, which may be attributed to the following reasons:

1. The superhydrophobic surface with rough structure can trap air in the surface texture, so that the droplets on the surface are in a non-wetting Cassie-Baxter state. The trapped air minimizes the interaction between the liquid droplet and the solid surface, and the water droplet easily slips off the surface when the surface is slightly inclined. Under actual freezing conditions, if water droplets fall from the surface due to gravity, there is no surface icing.
2. The large amount of air present in the superhydrophobic surface structure can become a good heat insulating layer to prevent the droplets from freezing, thereby delaying the time for the droplets to reach the nucleation temperature.
3. The existence of "cavitation" can reduce the chance of non-uniform nucleation of ice crystals.
4. The superhydrophobic surface can reduce the adhesion of the ice layer. The adhesion and wettability of the ice layer on the superhydrophobic surface are related to the value $(1 + \cos\theta_R)$. (θ_R = CA-SA) When the retreat angle θ_R of the droplets on the solid surface is greater than 118.2°, the adhesion of the ice layer will decrease significantly [37].

3.4 Robustness, Durability

We studied the effect of coating composition on the wettability and mechanical strength of ZnO/SiO_2 multi-scale coatings. The superhydrophobic properties of the prepared surface are mainly attributed to the synergistic effect of nano-scale and micro-scale surface roughness and low surface energy $-CF_2$ and $-CF_3$ groups. The surface coated with the ZnO/SiO_2 multi-scale coating exhibits excellent superhydrophobicity and has a stable Cassie-Baxtex morphology with a CA of 153° and SA of 3.3°. In addition to glass slides, ZnO/SiO_2 coatings are also applied to a variety of surfaces, including wind turbine blade, stainless steel plates, papers, plastics, and cotton cloth. All surfaces become superhydrophobic. Therefore, the coating can be applied to various materials, and the application prospect is very broad.

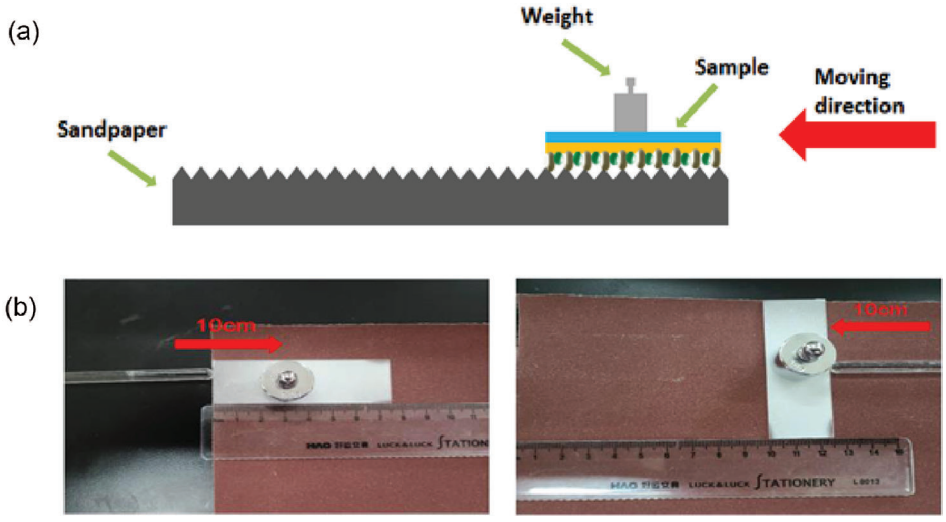

Figure 10: Schematic diagram of sandpaper abrasion experiment: (a) experimental diagram, and (b) experimental operation diagram

In the daily practical application, the actual focus of the development of anti-icing coatings is still the durability and stability in harsh environments. In order to verify the mechanical stability of the ZnO/SiO_2

coating, a sandpaper abrasion test was performed on the coating [38,39], as shown in Fig. 10. First, the samples coated with ZnO/SiO_2 were placed face down on SiC sandpaper. Then put 50 g weight on the coated sample, push the coated sample onto the sandpaper, and move 10 cm along the scale through the glass rod. Finally, the sample was rotated 90° and moved 10 cm in the opposite direction of the dial. Through the above three abrasion steps in the horizontal and vertical directions, the coating sample was subjected to a cycle of abrasion experiment. Figs. 11a and 11b show the changes of CA and SA of the coating samples as the test cycle increases. Fig. 11c shows the optical micrographs of the three coated samples after 10 sandpaper abrasion experiments. After 10 cycles of wear, CA decreased from 153° to 141°, and SA increased from 3.3° to 6.8°, but not more than 10°, indicating that even after the sandpaper was cyclically worn, it still maintained excellent hydrophobic properties. The coating can maintain such excellent characteristics mainly due to the micro-nano structure constructed by the mixture of multi-scale ZnO and SiO_2 nanoparticles, and the modified ZnO and SiO_2 nanoparticles have extremely low surface energy.

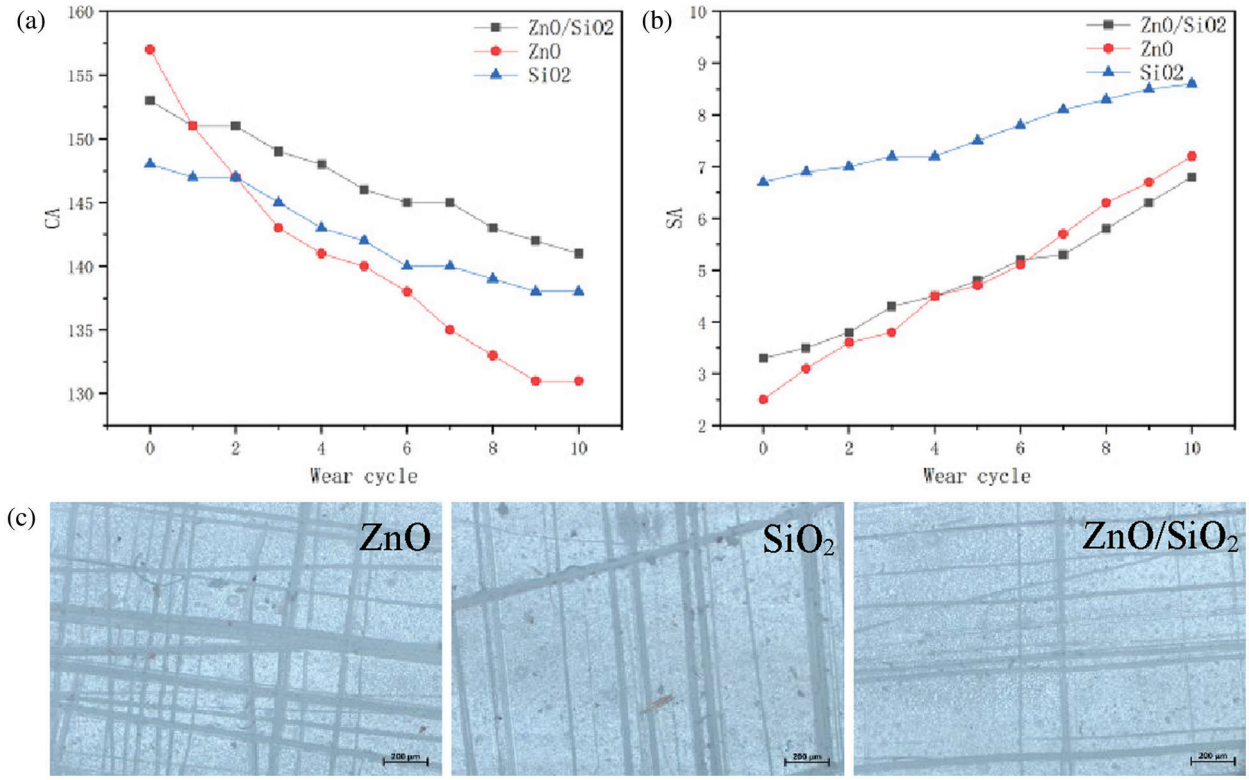

Figure 11: Data analysis of sandpaper abrasion experiment: (a) CA change of sandpaper abrasion experiment, (b) SA change of sandpaper abrasion experiment, and (c) Optical micrographs of the three coated samples after the sandpaper abrasion experiment

4 Conclusion

In this paper, on the basis of modifying ZnO and SiO_2 nanoparticles of different scales, a mechanically flexible ZnO/SiO_2 multi-scale micro-nano structure superhydrophobic anti-icing coating was directly constructed by the embedding method. The preparation process of the coating is simple. In addition to its high superhydrophobicity (CA is 153°, SA is 3.3°), the prepared surface also exhibits excellent mechanical durability and self-cleaning performance, which can resist the actual application of machinery damage. At the same time, the surface of the ZnO/SiO_2 coating exhibits excellent anti-icing ability under

low temperature and high humidity conditions, which can effectively delay the formation of ice. This is mainly due to the modification of ZnO and SiO_2, the different scales of ZnO and SiO_2 particles, and the synergistic effect of the micro-nano structure constructed by PDMS. Since the preparation process is simple, the cost is low, and it is suitable for a variety of substrates, it is expected to have great application prospects, such as wind turbine blade. This paper proposes a superhydrophobic coating with good mechanical flexibility in outdoor facilities and structures, as well as excellent self-cleaning and anti-icing properties.At the same time, this research has problems in the repairability of superhydrophobic anti-icing coatings and the anti-icing effect in extreme low temperature environments, which need to be further studied.

Acknowledgement: The authors gratefully acknowledge financial support from the Changsha University of Science and Technology Research and Innovation Project (CX2019SS21) and the National Energy Group Technology Innovation Project (HJLFD-QTHT-2019-09).

Funding Statement: This work was funded by the Changsha University of Science and Technology Research and Innovation Project (CX2019SS21) and the National Energy Group Technology Innovation Project (HJLFD-QTHT-2019-09).

Conflicts of Interest: The authors declare that they have no conflicts of interest to report regarding the present study.

References

1. Ayoub, H., Banihani, E. (2020). Performance and cost analysis of energy production from offshore wind turbines. *Energy Engineering, 117(1),* 41–47. DOI 10.3390/en10111904.
2. Jia, Y., Cheng, B., Li, X., Zhang, H., Dong, Y. (2020). Research on effect of icing degree on performance of NACA4412 airfoil wind turbine. *Energy Engineering, 117(6),* 413–427. DOI 10.32604/EE.2020.012019.
3. Zhang, S., Huang, J., Chen, Z., Lai, Y. (2017). Bioinspired special wettability surfaces: From fundamental research to water harvesting applications. *Small, 13(3),* 1602992. DOI 10.1002/smll.201602992.
4. Latthe, S. S., Sutar, R. S., Kodag, V. S., Bhosale, A. K., Kumar, A. M. et al. (2019). Self-cleaning superhydrophobic coatings: Potential industrial applications. *Progress in Organic Coatings, 128,* 52–58. DOI 10.1016/j.porgcoat.2018.12.008.
5. Golovin, K., Dhyani, A., Thouless, M. D., Tuteja, A. (2019). Low–interfacial toughness materials for effective large-scale deicing. *Science, 364(6438),* 371–375. DOI 10.1126/science.aav1266.
6. Golovin, K., Tuteja, A. (2017). A predictive framework for the design and fabrication of icephobic polymers. *Science Advances, 3(9),* e1701617. DOI 10.1126/sciadv.1701617.
7. Chen, C., Weng, D., Mahmood, A., Chen, S., Wang, J. (2019). Separation mechanism and construction of surfaces with special wettability for oil/water separation. *ACS Applied Materials & Interfaces, 11(11),* 11006–11027. DOI 10.1021/acsami.9b01293.
8. Liu, Y. C., Huang, W. J., Wu, S. H., Lee, M., Yeh, J. M. et al. (2018). Excellent superhydrophobic surface and anti-corrosion performance by nanostructure of discotic columnar liquid crystals. *Corrosion Science, 138,* 1–7. DOI 10.1016/j.corsci.2018.03.044.
9. Schellenberger, F., Encinas, N., Vollmer, D., Butt, H. J. (2016). How water advances on superhydrophobic surfaces. *Physical Review Letters, 116(9),* 096101. DOI 10.1103/PhysRevLett.116.096101.
10. Pan, R., Cai, M., Liu, W., Luo, X., Chen, C. et al. (2019). Extremely high cassie–Baxter state stability of superhydrophobic surfaces via precisely tunable dual-scale and triple-scale micro–nano structures. *Journal of Materials Chemistry a, 7(30),* 18050–18062. DOI 10.1039/C9TA04484A.
11. Jing, X., Guo, Z. (2018). Biomimetic super durable and stable surfaces with superhydrophobicity. *Journal of Materials Chemistry A, 6(35),* 16731–16768. DOI 10.1039/C8TA04994G.

12. Dalawai, S. P., Aly, M. A. S., Latthe, S. S., Xing, R., Sutar, R. S. et al. (2020). Recent advances in durability of superhydrophobic self-cleaning technology: A critical review. *Progress in Organic Coatings, 138,* 105381. DOI 10.1016/j.porgcoat.2019.105381.
13. Dai, S., Zhu, Y., Gu, Y., Du, Z. (2019). Biomimetic fabrication and photoelectric properties of superhydrophobic ZnO nanostructures on flexible PDMS substrates replicated from rose petal. *Applied Physics A, 125(2),* 1–11. DOI 10.1007/s00339-019-2438-7.
14. Zhou, H., Chen, R., Liu, Q., Liu, J., Yu, J. et al. (2019). Fabrication of ZnO/epoxy resin superhydrophobic coating on AZ31 magnesium alloy. *Chemical Engineering Journal, 368,* 261–272. DOI 10.1016/j.cej.2019.02.032.
15. Zhang, X. F., Chen, Y. Q., Hu, J. M. (2020). Robust superhydrophobic SiO_2/polydimethylsiloxane films coated on mild steel for corrosion protection. *Corrosion Science, 166,* 108452. DOI 10.1016/j.corsci.2020.108452.
16. Wang, M., Tan, X., Tu, Y., Xiang, P., Jiang, L. et al. (2020). Self-healing PDMS/SiO_2-$CaCO_3$ composite coating for highly efficient protection of building materials. *Materials Letters, 265,* 127290. DOI 10.1016/j.matlet.2019.127290.
17. Lu, Y., Sathasivam, S., Song, J., Crick, C. R., Carmalt, C. J. et al. (2015). Robust self-cleaning surfaces that function when exposed to either air or oil. *Science, 347(6226),* 1132–1135. DOI 10.1126/science.aaa0946.
18. Li, Z., Cao, M., Li, P., Zhao, Y., Bai, H. et al. (2019). Surface-embedding of functional micro-/nanoparticles for achieving versatile superhydrophobic interfaces. *Matter, 1(3),* 661–673. DOI 10.1016/j.matt.2019.03.009.
19. Kim, D., Sasidharanpillai, A., Yun, K. H., Lee, Y., Yun, D. J. et al. (2019). Assembly mechanism and the morphological analysis of the robust superhydrophobic surface. *Coatings, 9(8),* 472. DOI 10.3390/coatings9080472.
20. Zhang, X., Si, Y., Mo, J., Guo, Z. (2017). Robust micro-nanoscale flowerlike ZnO/epoxy resin superhydrophobic coating with rapid healing ability. *Chemical Engineering Journal, 313,* 1152–1159. DOI 10.1016/j.cej.2016.11.014.
21. Peng, C., Chen, Z., Tiwari, M. K. (2018). All-organic superhydrophobic coatings with mechanochemical robustness and liquid impalement resistance. *Nature Materials, 17(4),* 355–360. DOI 10.1038/s41563-018-0044-2.
22. Xu, H., Shi, Y., Yang, S., Li, B. (2019). A linear molecule sulfur-rich organic cathode material for high performance lithium–sulfur batteries. *Journal of Power Sources, 430,* 210–217. DOI 10.1016/j.jpowsour.2019.05.022.
23. Tao, C., Zhang, L. (2020). Fabrication of multifunctional closed-surface SiO_2-TiO_2 antireflective thin films. *Colloids and Surfaces A: Physicochemical and Engineering Aspects, 585,* 124045. DOI 10.1016/j.colsurfa.2019.124045.
24. Li, S., Zhou, H., Xiao, L., Fan, J., Zheng, X. (2019). Fabrication of super-hydrophobic titanosilicate Sub-micro sphere with enhanced epoxidation catalytic activity. *Catalysis Letters, 149*,*(5),* 1396–1402. DOI 10.1007/s10562-019-02720-y.
25. Patil, G. D., Patil, A. H., Jadhav, S. A., Patil, C. R., Patil, P. S. (2019). A new method to prepare superhydrophobic cotton fabrics by post-coating surface modification of ZnO nanoparticles. *Materials Letters, 255,* 126562. DOI 10.1016/j.matlet.2019.126562.
26. Gao, X., Jiang, L. (2004). Water-repellent legs of water striders. *Nature, 432(7013),* 36–36. DOI 10.1038/432036a.
27. Shao, Y., Zhao, J., Fan, Y., Wan, Z., Lu, L. et al. (2020). Shape memory superhydrophobic surface with switchable transition between "Lotus effect" to "Rose petal effect". *Chemical Engineering Journal, 382,* 122989. DOI 10.1016/j.cej.2019.122989.
28. Chen, C., Liu, M., Zhang, L., Hou, Y., Yu, M. et al. (2019). Mimicking from rose petal to lotus leaf: Biomimetic multiscale hierarchical particles with tunable water adhesion. *ACS Applied Materials & Interfaces, 11(7),* 7431–7440. DOI 10.1021/acsami.8b21494.
29. Yong, J., Chen, F., Yang, Q., Huo, J., Hou, X. (2017). Superoleophobic surfaces. *Chemical Society Reviews, 46(14),* 4168–4217. DOI 10.1039/C6CS00751A.
30. Sun, Y., Guo, Z. (2019). Recent advances of bioinspired functional materials with specific wettability: From nature and beyond nature. *Nanoscale Horizons, 4(1),* 52–76. DOI 10.1039/C8NH00223A.

31. Tan, Y., Hu, B., Chu, Z., Wu, W. (2019). Bioinspired superhydrophobic papillae with tunable adhesive force and ultralarge liquid capacity for microdroplet manipulation. *Advanced Functional Materials, 29(15),* 1900266. DOI 10.1002/adfm.201900266.
32. Zhang, K., Li, Z., Maxey, M., Chen, S., Karniadakis, G. E. (2019). Self-cleaning of hydrophobic rough surfaces by coalescence-induced wetting transition. *Langmuir, 35(6),* 2431–2442. DOI 10.1021/acs.langmuir.8b03664.
33. Lafuma, A., Quéré, D. (2003). Superhydrophobic states. *Nature Materials, 2(7),* 457–460. DOI 10.1038/nmat924.
34. Guo, T., Weng, X. (2019). Evaluation of the freeze-thaw durability of surface-treated airport pavement concrete under adverse conditions. *Construction and Building Materials, 206,* 519–530. DOI 10.1016/j.conbuildmat.2019.02.085.
35. Nine, M. J., Tung, T. T., Alotaibi, F., Tran, D. N. H., Losic, D. (2017). Facile adhesion-tuning of superhydrophobic surfaces between "lotus" and "petal" effect and their influence on icing and deicing properties. *ACS Applied Materials & Interfaces, 9(9),* 8393. DOI 10.1021/acsami.6b16444.
36. Zhao, J., Zhang, G., Dong, Z. Y., Scala, M. L. (2018). Robust forecasting aided power system state estimation considering state correlations. *IEEE Transactions on Smart Grid, 9(4),* 2658–2666. DOI 10.1109/TSG.2016.2615473.
37. Qi, C., Lei, X., Zhou, B., Wang, C., Zheng, Y. (2019). Temperature regulation of the contact angle of water droplets on the solid surfaces. *The Journal of Chemical Physics, 150(23),* 234703. DOI 10.1063/1.5090529.
38. Xu, P., Coyle, T. W., Pershin, L., Mostaghimi, J. (2019). Understanding the correlations between the mechanical robustness, coating structures and surface composition for highly-/super-hydrophobic ceramic coatings. *Surface and Coatings Technology, 378,* 124929. DOI 10.1016/j.surfcoat.2019.124929.
39. He, K., Chen, J. J., Weng, W. X., Li, C. C., Li, Q. (2018). Microstructure and mechanical properties of plasma sprayed Al_2O_3-ysz composite coatings. *Vacuum, 151,* 209–220. DOI 10.1016/j.vacuum.2018.01.038.